Effect of Field Line Expansion on the Energy Flux of Alfvén Waves in the Solar Atmosphere

1872 PRIFYSGOL ABERYSTWYTH UNIVERSITY
Science and Technology Facilities Council
Tahlina Borradaile *(tab22@aber.ac.uk)*, Yeghiazar Taroyan

1. Introduction

Recent studies have revealed Alfvén waves in the solar corona that have sufficient power to heat the solar corona. Alfvén waves have previously been shown to be highly reflective in the lower solar atmosphere, due to inhomogeneities, especially at lower frequencies. This indicates a gap in understanding. Previous studies have used simplified field geometries, such as the thin flux tube approximation, however this does not reflect reality of the solar atmosphere. By modelling the propagation of Alfvén waves along various magnetic field line geometries in a stratified atmosphere, we challenge the view that these motions are always strongly reflected. Certain geometries lead to a substantial improvement in energy transport by Alfvén waves.

2. Simulation Set-Up

The MHD equations of motion and induction are solved numerically to show the time evolution of velocity and magnetic perturbations of Alfvénic motions along magnetic field lines. The rate of expansion of the field lines are varied across three cases, similar to our analytical study (Taroyan & Borradaile, '24)

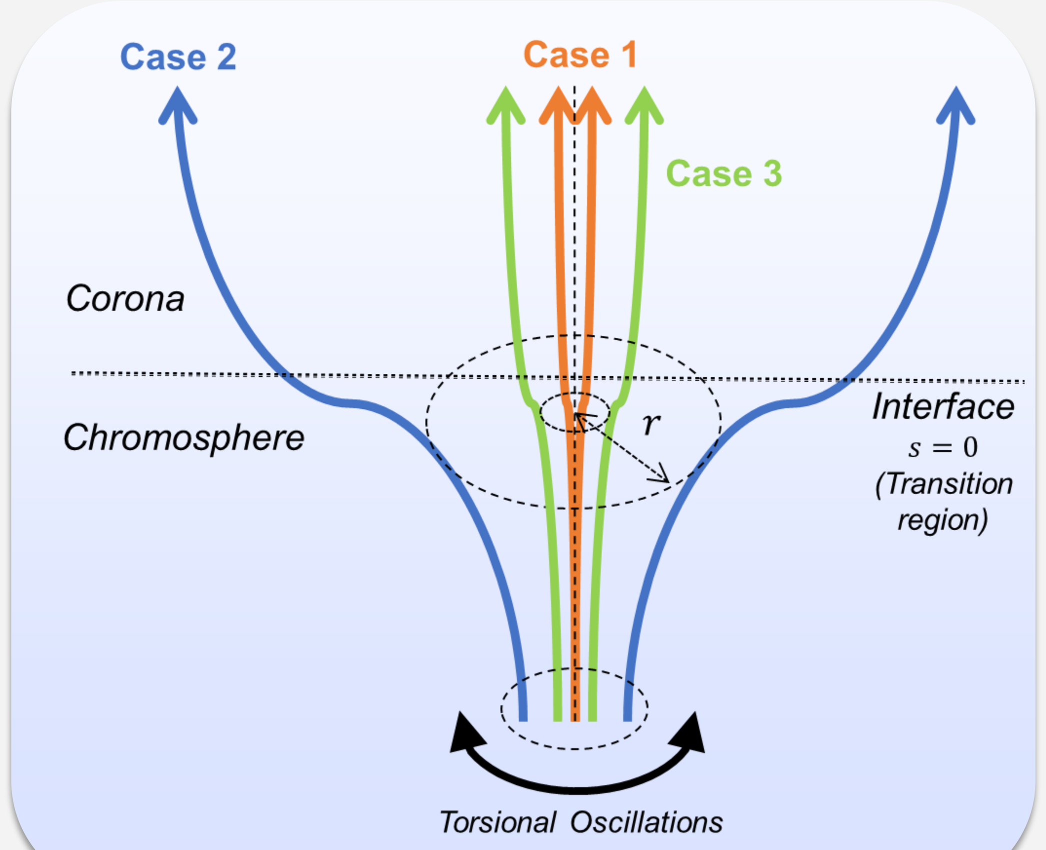

Fig. 1: Sketch of 2-layer model and three field line cases.

■ Case 1	■ Case 2	■ Case 3
Thin flux tube approximation	Highly divergent field lines	Moderately divergent field lines
Cut-off frequencies vanish		*No reflection*

- **2-layer model:** variable chromosphere ($s < 0$), constant corona ($s > 0$).
- **Background plasma quantities (B_0, c_A, ρ):** large variation governed by exponential profiles, but consistent across cases.
- **Expansion of field lines (r profile):** varied across cases.
- **Solver:** FDM MacCormack Method.
- **Boundaries:** open, no domain edge reflections.
- **Drivers:** pulse, sinusoidal, random (200 periodic events) in time. Gaussian in space.

3. Single Pulse Driver

Backward-going reflections, (secondary pulses in Fig.2) are seen at the wave source in cases 1 and 2, but not in case 3, indicating no reflection seen in case 3. Amplitudes and energy at the interface are larger for case 3.

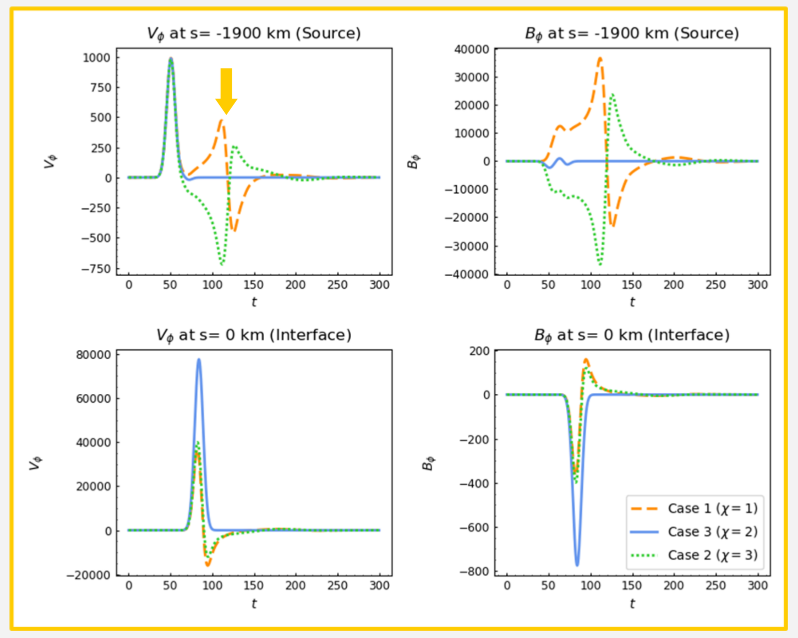

Fig. 2: Velocity and magnetic field perturbations at the wave source and the interface for the single pulse driver.

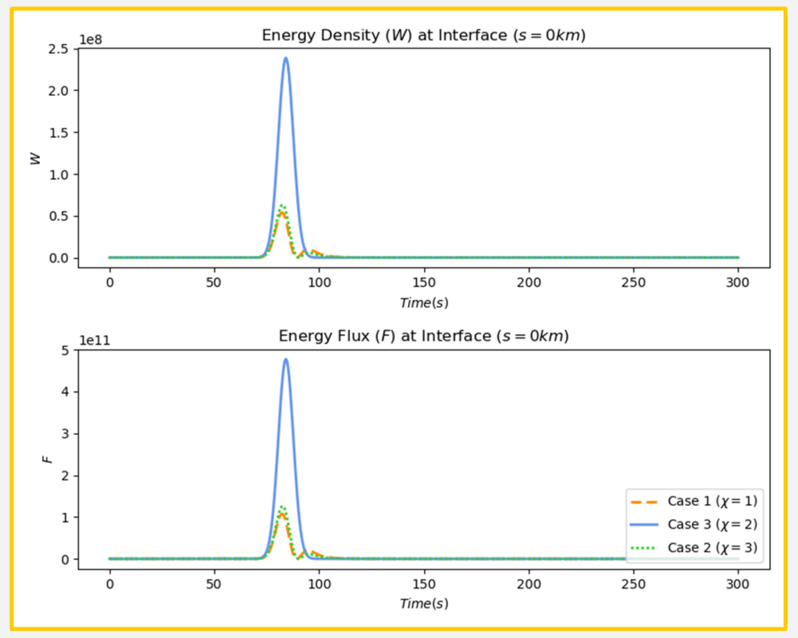

Fig. 3: Energy flux and density at the interface for the single pulse driver.

3. High vs Low Frequency

For the periodic driver - as frequency decreases, the amplitudes and energies of cases 1 and 2 at the interface are notably diminished. However for case 3, these stay the same regardless of frequency. This supports the idea of case 3 not experiencing any reflection, and cases 1 and 2 experiencing increased reflection as frequency decreases.

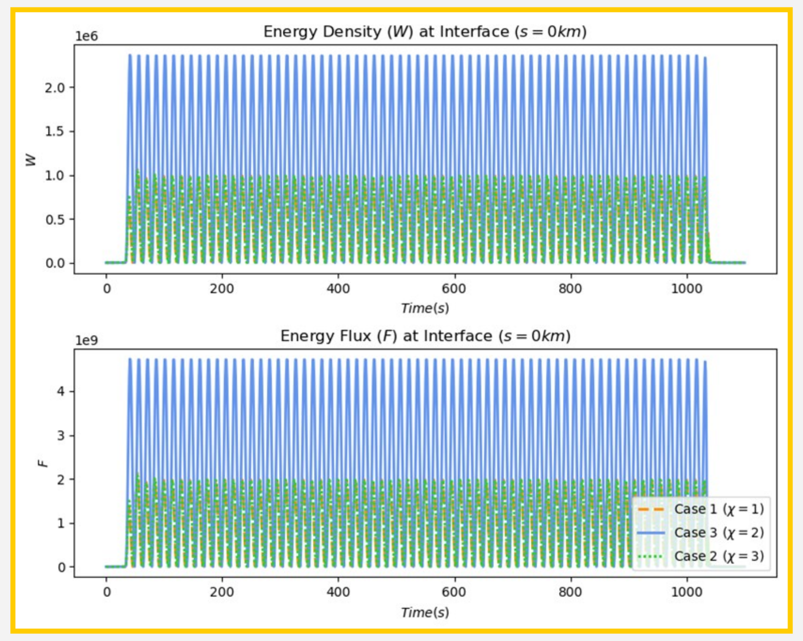

Fig. 4: Energy density and flux at the interface for the periodic driver of a period of 30s.

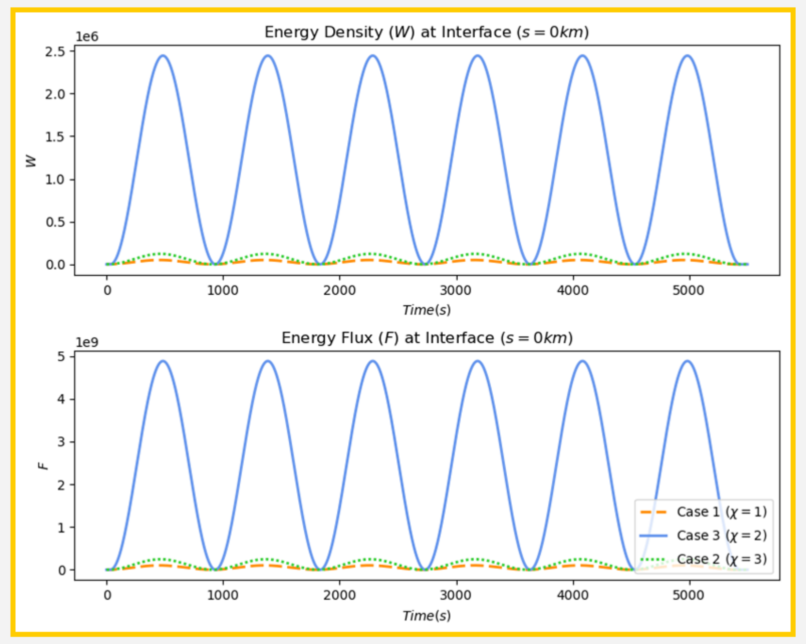

Fig. 5: Energy density and flux at the interface for the periodic driver of a period of 30m.

For references and more.
users.aber.ac.uk/ tab22

Analytical Study
Taroyan and Borradaile, A&A, 691 (2024) A55

4. Random Driver

An example of the noise generated by the driver is seen in Fig. 6. A similar trend is seen with the random driver, with case 3 showing profoundly larger amplitudes (Fig. 7) and energies (Fig. 8) at the interface compared with cases 1 and 2.

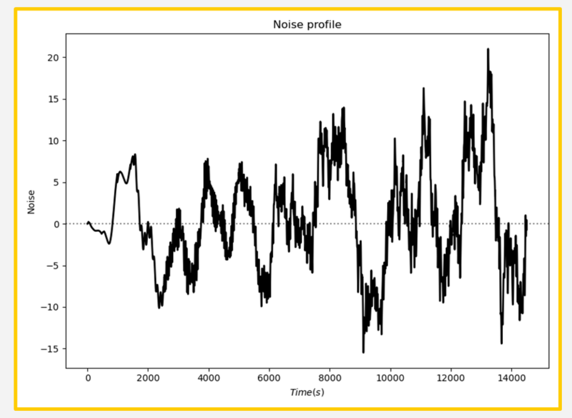

Fig. 6: Example of generated noise profile.

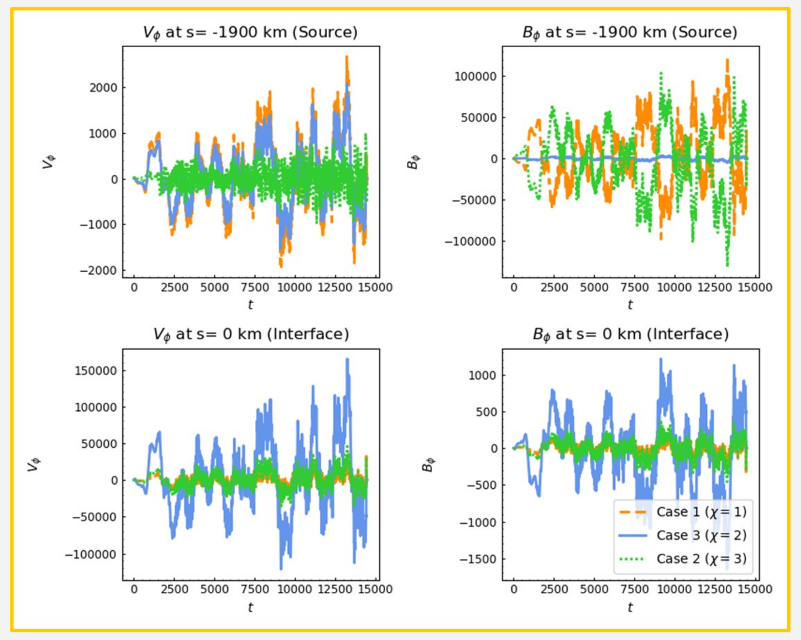

Fig. 7: Velocity and magnetic field perturbations at the wave source and the interface for the random driver.

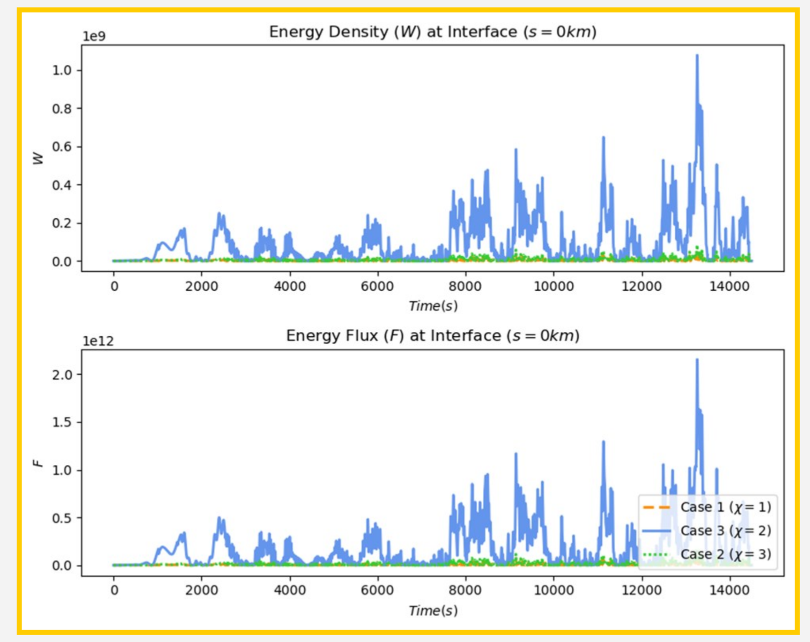

Fig. 8: Energy flux and density at the interface for the random driver.

The negative slope in the power spectrum is reminiscent of pink noise. In Fig. 9, it can be seen that overall, case 3 has a higher power across all frequencies. However, looking closely at the three cases, a convergence is seen at higher frequencies, which corresponds to a reduced power of cases 1 and 2 at lower frequencies.

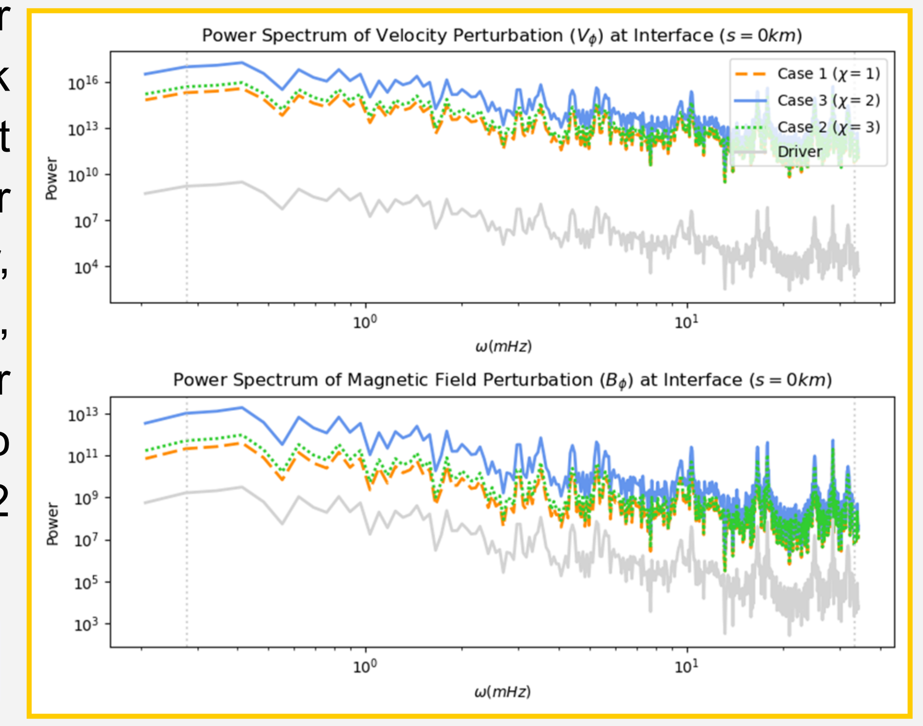

Fig. 9: Power spectra at the interface for the three cases, and at the source for the driver.

6. Conclusions

Numerical techniques have been used to **simulate the propagation of Alfvén waves** in the solar atmosphere for **three different geometries**. In **low and high expansion** cases (1, 2), an **increase in reflection** is seen **as frequency lowers**, heavily **suppressing wave flux**. In the **mid expansion case** (3), **no reflection** is seen, resulting in a **strong upward flux** at the transition region.

Similarly to our previous study, it was found that the **expansion rate of field lines** is a key contributor to how much **energy to transmitted into the corona**.

The next step in this work is moving to a **potential field model**, expanding on Hollweg et. al.'s 1982 equations, to further investigate the relationship between the **field line geometry** and the **flux** seen at the **transition region**.